The Added Value of [^{68}Ga]Ga-DOTA-FAPI-04 PET/CT in Patients with Head and Neck Cancer of Unknown Primary with [^{18}F]FDG Negative Findings

Bingxin Gu
Fudan University Shanghai Cancer Center
Xiaoping Xu
Fudan University Shanghai Cancer Center
Ji Zhang
Fudan University Shanghai Cancer Center
Xiaomin Ou
Fudan University Shanghai Cancer Center
Zuguang Xia
Fudan University Shanghai Cancer Center
Qing Guan
Fudan University Shanghai Cancer Center
Silong Hu
Fudan University Shanghai Cancer Center
Zhongyi Yang
Fudan University Shanghai Cancer Center
Shaoli Song (shaoli-song@163.com)
Fudan University Shanghai Cancer Center https://orcid.org/0000-0003-2544-7522

Research Article

Keywords: [68Ga]Ga-DOTA-FAPI-04, Head and neck, Cancer of unknown primary, Metastases

Posted Date: May 28th, 2021

DOI: https://doi.org/10.21203/rs.3.rs-530004/v1

Abstract

Purpose [^{18}F]fluorodeoxyglucose ([^{18}F]FDG) positron emission tomography/computed tomography (PET/CT) plays an important role in location of primary tumor for patients with head and neck cancer of unknown primary (HNCUP). But sometimes, [^{18}F]FDG PET/CT still cannot find the primary malignancy. As ^{68}Ga-radiolabeled fibroblast activation protein inhibitor (FAPI) PET/CT has promising results in detecting different tumor entities, our study aimed to evaluate the performance of [^{68}Ga]Ga-DOTA-FAPI-04 PET/CT for detecting the primary tumor in HNCUP patients with negative [^{18}F]FDG findings.

Methods A total of eighteen patients (16 males and 2 females; median age, 55 years; range, 24-72 years) with negative [^{18}F]FDG findings were eligible in this study. All patients underwent [^{18}F]FDG and [^{68}Ga]Ga-DOTA-FAPI-04 PET/CT within one week. Biopsy and histopathological examinations were done in the sites with positive [^{68}Ga]Ga-DOTA-FAPI-04 PET/CT findings.

Results [^{68}Ga]Ga-DOTA-FAPI-04 PET/CT detected the primary tumor in 7 of 18 patients (38.89%). The primary tumors sites were in nasopharynx (1/7), palatine tonsil (2/7), submandibular gland (2/7), and hypopharynx (2/7). The primary tumors showed mild to intensive uptake of FAPI (mean SUV_{max}, 8.79; range, 2.60-16.50) and excellent tumor-to-contralateral normal tissue ratio (mean SUV_{max} ratio, 4.50; range, 2.17-8.21). In lesion-based analysis, a total of 65 lymph nodes and 17 bone metastatic lesions were identified. The mean SUV_{max} of lymph node metastases were 9.05 ± 5.29 for FDG and 9.08 ± 4.69 for FAPI (p = 0.975); as for bone metastases, the mean SUV_{max} were 8.11 ± 3.00 for FDG and 6.96 ± 5.87 for FAPI, respectively (p = 0.478). The mean tumor-to-background ratio (TBR) values of lymph node and bone metastases were 10.65 ± 6.59 vs. 12.80 ± 8.11 (p = 0.100) and 9.08 ± 3.35 vs. 9.14 ± 8.40 (p = 0.976), respectively.

Conclusion We present first evidence of diagnostic role of [^{68}Ga]Ga-DOTA-FAPI-04 PET/CT in HNCUP, and our study demonstrated that [^{68}Ga]Ga-DOTA-FAPI-04 PET/CT had the potential to improve the detection rate of primary tumor in HNCUP patients with negative FDG findings. Moreover, [^{68}Ga]Ga-DOTA-FAPI-04 had similar performance in assessing metastases with [^{18}F]FDG.

Introduction

Head and neck cancer of unknown primary (HNCUP) is defined as a metastatic disease in the cervical lymph nodes with an unidentifiable primary tumor [1], even after a thorough diagnostic workup according to the National Comprehensive Cancer Network (NCCN) [2] and American Society of Clinical Oncology (ASCO) guidelines [3]. HNCUP constitutes 1-5% of all head and neck cancers [4-6]. Squamous cell carcinoma (SCC) is the most common pathological type of HNCUP, and approximately 90% of these cases are associated with human papillomavirus (HPV) [1]. The most frequent primary site of HNCUP is oropharynx, accounting for 80-90% [7]. However, some factors, like small tumor volume, hidden location, slow growth rate, and tumor involution, hinder primary site identification. The absence of primary tumor may result in uncertain treatment decisions and increasing psychological burden for patients with HNCUP.

Medical imaging plays an important role in oncology, particularly in tumor location [8]. Conventional imaging modalities, Computed Tomography (CT) and Magnetic Resonance Imaging (MRI), can provide plentiful anatomical information about primary and metastatic malignancies, including anatomic situation, extracapsular

extension, and contralateral lesions. However, the detection rates of primary site for these two imaging modalities range from 9 to 23% in HNCUP [9-11]. Positron emission tomography/computed tomography (PET/CT), a typical molecular imaging modality, outperforms CT and MRI in identifying primary tumor with a detection rate of 25-69% by using [^{18}F]fluorodeoxyglucose ([^{18}F]FDG) [12-15]. Nevertheless, some limitations hamper the application of [^{18}F]FDG PET/CT in primary tumor identification for HNCUP [16, 17]. Firstly, physiological FDG uptake can be seen in any lymphatic structure (especially Waldeyer's ring), salivary glands, and brown fat. Secondly, symmetrical vocal cords and neck muscles uptake are commonly seen if the patient talks or coughs during the uptake period. Thirdly, infection and chronic inflammation (i.e., nasopharyngitis, amygdalitis, and gingivitis) can also result in high FDG uptake. These three limitations may lead to false positive findings with a rate of 16-25% [4, 12, 15]. Last but not least, false negative FDG uptake can be seen in small, mucinous, well-differentiated, and necrotic lesions [17]. Therefore, novel specific radiopharmaceuticals with low background uptake in head and neck, which may better improve the detection rate of primary tumor in HNCUP, are in urgent need.

Cancer associated fibroblasts (CAFs), accounting for high proportion of most solid tumor mass, plays a vital role in tumor growth, migration, and progression [18]. The major feature to discriminate CAFs from normal fibroblast is the overexpression of fibroblast activation protein (FAP) [19]. FAP is a type II membrane-bound glycoprotein belonging to the dipeptidyl peptidase 4 family [20]. The presence of FAP was observed on a variety of epithelial and mesenchymal malignancies [21, 22]. Recently, ^{68}Ga-radiolabeled fibroblast activation protein inhibitor (FAPI), a novel FAP-targeted PET tracer, has shown great value in diagnosis of diverse carcinomas, including well-differentiated cancers [23-25]. Furthermore, some studies [26, 27] demonstrated that [^{68}Ga]Ga-DOTA-FAPI revealed high uptake in primary tumors and low background noise of the head and neck region. These promising findings indicate [^{68}Ga]Ga-DOTA-FAPI could serve as a potential alternative to [^{18}F]FDG for the assessment of head and neck cancers.

Thus, the aim of this study was to investigate the value of [^{68}Ga]Ga-DOTA-FAPI-04 PET/CT in identifying primary tumor of FDG-negative HNCUP.

Materials And Methods

Patient selection

All patients included in this study were diagnosed with metastatic cervical carcinoma by fine-needle aspiration (FNA). [^{18}F]FDG and [^{68}Ga]Ga-DOTA-FAPI-04 PET/CT were recommended to them for identifying primary tumor based on decision from multidisciplinary team (MDT) of head and neck cancer. For further investigate the role of [^{68}Ga]Ga-DOTA-FAPI-04 PET/CT in HNCUP, inclusion criteria were as follows: (i) adult patients (age > 18 and < 80 years); (ii) pathology conformed metastatic cervical carcinoma; (iii) conventional imaging modalities couldn't provide positive finding of primary tumor; (vi) both [^{18}F]FDG and [^{68}Ga]Ga-DOTA-FAPI-04 PET/CT were performed. The exclusion criteria were (i) patients with lymphomas or non-head and neck original cancers, confirmed by immunohistochemistry (IHC); (ii) patients with suspected primary lesion by [^{18}F]FDG PET/CT, confirmed by subsequent histologic examination; (iii) patients with two or more malignant tumors history; (vi) patients unwilling to take [^{18}F]FDG or [^{68}Ga]Ga-DOTA-FAPI-04 PET/CT.

A total of thirty-two patients were enrolled from our center between June 2020 to Feb 2021. However, among these patients, three were diffuse large B-cell lymphoma (DLBCL), three were lung origin, one was digestive

system origin, one was female reproductive system origin, and six were with both positive [^{18}F]FDG and [^{68}Ga]Ga-DOTA-FAPI-04 PET/CT findings. All patients had biopsies of the sites with positive PET/CT findings for primary tumors. For these patients without clear primary tumor site after PET/CT scan, a three-month follow-up was performed. The metastatic lesions were defined by pathology, imaging findings, and follow-up. The data of demographics were collected. This study was approved by Fudan University Shanghai Cancer Center Institutional Review Board (ID 2004216-25) conducted in accordance with the 1964 Declaration of Helsinki and its later amendments or comparable ethical standards, and all subjects signed an informed consent form.

Radiopharmaceuticals and PET/CT scanning procedure

[^{18}F]FDG was produced automatically using Explora FDG_4 module with cyclotron (Siemens CTI RDS Eclips ST, Knoxville, Tennessee, USA) in our center. DOTA-FAPI-04 were obtained commercially (Jiangsu Huayi Technology CO., LTD, Jiangsu, China). DOTA-FAPI-04 was radiolabeled with ^{68}Ga according to Lindner et al [28]. Briefly, the DOTA-FAPI-04 and ^{68}Ga-solution (elution with 0.5M HCl) were mixed with sodium acetate, and the pH was maintained about 4.5. Then the reaction mixture was heated to 100 ℃ for 20 min. The [^{68}Ga]Ga-DOTA-FAPI-04 was obtained by solid phase extraction. Radiochemical purity of [^{18}F]FDG and [^{68}Ga]Ga-DOTA-FAPI-04 were both over 95%.

[^{18}F]FDG and [^{68}Ga]Ga-DOTA-FAPI-04 PET/CT were performed within one week. For [^{18}F]FDG PET/CT scanning, patients were fasted at least 6 hours, maintaining venous blood glucose levels under 10 mmol/L prior to [^{18}F]FDG administration. But this was not necessary for [^{68}Ga]Ga-DOTA-FAPI-04 PET/CT scanning. After injecting with 260.64 ± 40.81 MBq (range, 188.03-335.36 MBq) of [^{18}F]FDG or 143.71 ± 16.19 MBq (range, 108.56-165.83 MBq) of [^{68}Ga]Ga-DOTA-FAPI-04, patients were kept in a quiet environment for approximately 60 mins prior to examination. All images were obtained on a Biograph mCT Flow scanner (Siemens Medical Solutions). Low-dose CT scanning was first performed for location: scanning ranging from the proximal thighs to head, with 120 kV, 100 mAs, CARE Dose4D, slice thickness 3 mm, increment 2 mm, pitch 1.0, rotation time 0.5s, soft-tissue reconstruction kernel. Immediately after CT scanning, a PET emission scan that covered the corresponding field of CT was acquired in 3-dimensional mode using FlowMotion with a speed of 2. The emission data were corrected for random, scatter and decay. PET image data sets were reconstructed iteratively using an ordered-subset expectation maximization iterative reconstruction (OSEM) by applying CT data for attenuation correction. Fusion images were reviewed and manipulated on a multimodality computer platform (Syngo, Siemens, Knoxville, Tennessee, USA). Two experienced nuclear medicine physicians analyzed and interpreted the images independently, and they reached a consensus in case of inconsistency.

For quantitative analysis, maximum or mean of standardized uptake value (SUV) normalized to body weight were manually computed for tumor lesions and healthy tissues by drawing a 3-dimensional volume of interest (VOI). Meanwhile, SUV_{max} ratio for primary tumor was defined as the quotient of the SUV_{max} of primary tumor and the contralateral normal tissue, and tumor-to-background ratio (TBR) for tumor lesions was calculated according to the formula: $TBR = tSUV_{max}/bSUV_{mean}$, where $tSUV_{max}$ is the maximum SUV of tumor lesion, and $bSUV_{mean}$ is the mean SUV of muscle.

Statistical analyses

All statistical analyses were performed using SPSS 25.0 (IBM, Armonk, NY, USA). Means with standard deviation (SD) or medians with ranges were used to describe continuous characteristics. To compare the uptake of [^{18}F]FDG and [^{68}Ga]Ga-DOTA-FAPI-04 in metastatic lesions, two-sample t tests were used. Two-tailed $p < 0.05$ were considered statistically significant.

Results

Patients

From June 2020 to April 2021, there were eighteen patients with HNCUP were eligible for this study according to the inclusion and exclusion criterion (Fig. 1). The basic clinical characteristics were presented in Table 1. Among the included eighteen patients (16 males and 2 females; median age, 55 years; range, 24-72 years), two (11.11%) were infected with Epstein-Barr virus (EBV); six (33.33%) were infected with HPV; sixteen (88.89%) were pathologically diagnosed with cervical lymph node SCC and two (11.11%) were adenocarcinoma (AC).

Comparison of [^{18}F]FDG and [^{68}Ga]Ga-DOTA-FAPI-04 PET/CT semiquantitative parameters in metastatic lesions

A total of 65 lymph node and 17 bone metastases were detected by both [^{18}F]FDG and [^{68}Ga]Ga-DOTA-FAPI-04 PET/CT (Fig.2 and Table 2). Both tracers showed intensive uptake in lymph node and bone metastases. The mean SUV_{max} value of lymph node metastases was 9.05 ± 5.29 for FDG and 9.08 ± 4.69 for FAPI ($p = 0.975$). In case of TBR, FAPI was a litter higher than FDG (12.80 ± 8.11 and 10.65 ± 6.59, respectively). But the difference was not significant ($p = 0.100$). For bone metastases, the mean SUV_{max} value was 8.11 ± 3.00 for FDG and 6.96 ± 5.87 for FAPI ($p = 0.478$), and the mean TBR value was 9.08 ± 3.35 and 9.14 ± 8.40 ($p = 0.976$), respectively. Generally, no significant uptake difference was observed between FDG and FAPI in lymph node and bone metastases, indicating that [^{68}Ga]Ga-DOTA-FAPI-04 PET/CT had similar performance as [^{18}F]FDG PET/CT in assessing metastases of head and neck cancers.

[^{68}Ga]Ga-DOTA-FAPI-04 PET/CT imaging results of primary tumors

Among these FDG-negative patients, a total of seven patients (38.89%) identified primary tumors by [^{68}Ga]Ga-DOTA-FAPI-04 PET/CT, pathologically confirmed by subsequent biopsy. In terms of pathological type, [^{68}Ga]Ga-DOTA-FAPI-04 PET/CT showed a higher detection rate in adenocarcinoma (2/2, 100%) than SCC (5/16, 31.25%). For the location of primary tumor, one was in nasopharynx, two were in palatine tonsil (Fig. 3), two were in submandibular gland (Fig. 4), and two were in hypopharynx (Fig.5 and Table 3). In patient 2 (Fig. 3), right and left palatine tonsil showed similar uptake of FDG (SUV_{max} = 6.4 and 6.0, respectively), with a SUV_{max} ratio of 1.07 (1.04 for patient 3). But [^{68}Ga]Ga-DOTA-FAPI-04 PET/CT only showed intensive uptake in right palatine tonsil (SUV_{max} = 8.30), markedly higher than the contralateral palatine tonsil (SUV_{max} ratio = 3.46).

According to the 8th edition American Joint Committee on Cancer (AJCC) TNM staging classification, the TNM stage for these seven patients ranged from I to IVC. The smallest primary tumor size detected by [^{68}Ga]Ga-DOTA-FAPI-04 PET/CT was 5 ´ 3 mm. The mean SUV_{max} value of [^{68}Ga]Ga-DOTA-FAPI-04 for primary tumors was 8.79 (rang, 2.60-16.50), and the mean TBR value was 11.50 (range, 2.36-27.50). When compared to the contralateral normal tissue, primary tumor showed a remarkable higher uptake of FAPI, with a mean SUV_{max} ratio of 4.50 (range, 2.17-8.21).

Discussion

Identifying the primary tumor remains a concern for patients with HNCUP, though the development in imaging, endoscope, and pathology techniques. If without any positive findings by non-invasive procedures, invasive diagnostic operations, like tonsillectomy, are performed with a risk of bleeding or infection [5]. Thus, novel non-invasive methods may be needed for improving detection rate of primary tumor in HNCUP patients. This study took advantage of trials to investigate the performance of [^{68}Ga]Ga-DOTA-FAPI-04 PET/CT in identifying primary tumor of FDG-negative HNCUP. Our results demonstrated that [^{68}Ga]Ga-DOTA-FAPI-04 PET/CT can dramatically improve the detection rate of primary tumor in HNCUP patients comparing to [^{18}F]FDG PET/CT. Furthermore, [^{68}Ga]Ga-DOTA-FAPI-04 may compare favorably to ^{18}F-FDG in assessing metastases.

The current study exhibited a 38.89% (7/18) detection rate of primary tumor by [^{68}Ga]Ga-DOTA-FAPI-04 PET/CT. Notably, these patients were all with false negative [^{18}F]FDG PET/CT findings. The sites of false negative [^{18}F]FDG PET/CT findings in this study were nasopharynx, palatine tonsil, submandibular gland, and hypopharynx, which was different from previously reported observations that the tonsil was the most frequent false negative location [15]. Recently, S. Serfling et al [27] reported [^{68}Ga]Ga-DOTA-FAPI-04 PET/CT showed a better visual detection of the malignant primary in Waldeyer's tonsillar ring than [^{18}F]FDG PET/CT. However, the representative cases could provide positive findings of primary site by [^{18}F]FDG PET/CT alone in terms of HNCUP. Another previous research demonstrated that an SUV_{max} ratio of FDG uptake between tonsils of ³ 1.6 could be regarded as malignancy and used to guide biopsy [29]. In this study, two patients were diagnosed with palatine tonsil carcinoma by tonsillectomy. Puzzlingly, [^{18}F]FDG PET/CT revealed no visual difference between right and left palatine tonsils in both two cases. Furthermore, the SUV_{max} ratios of FDG uptake were all approximate equivalent to 1.00 (1.07 and 1.04 for patient 2 and 3, respectively), which was mistaken as physiologic uptake. By contrast, [^{68}Ga]Ga-DOTA-FAPI-04 PET/CT showed intensive uptake in tumor site and low uptake in the normal site, resulting in an obvious visual difference (SUV_{max} ratio = 3.46 and 8.21, respectively). In line with our results, M. Syed et al [26] demonstrated high FAPI avidity within tumorous lesions and low background uptake in healthy tissues of the head and neck region. In other ways, this study once again emphases the potential role of [^{68}Ga]Ga-DOTA-FAPI-04 PET/CT in detecting palatine tonsil carcinoma, particularly in FDG-negative patients.

In addition to high grade physiologic uptake of head and neck, small size of the lesions was the major reason for the false negative FDG findings due to the partial volume effect and low tumor glucose metabolic activity [30, 31]. In this study, [^{18}F]FDG PET/CT missed 3 of 7 primary tumors by reason of the small size (diameter < 10 mm). Encouragingly, [^{68}Ga]Ga-DOTA-FAPI-04 PET/CT revealed mild uptake (SUV_{max} = 2.60, 3.20, and 3.60 for patient 1, 6, and 7, respectively) and clearly visual difference (SUV_{max} ratio = 2.17, 2.91, and 3.27, respectively) in these primary tumors with small size, which was consistent with previous research [24]. The uptake of FAPI is mainly based on the expression of FAP on CAFs among solid tumor microenvironment. And even small primary tumors of T1 stage could show a moderate FAP expression [27]. Thus, [^{68}Ga]Ga-DOTA-FAPI-04 could serve as an alternative tracer for identifying primary tumor of small size to reduce the false negative results by [^{18}F]FDG PET/CT.

Most of the researches focus on SCC, as it is the most frequent pathological type of HNCUP [3-5]. However, some other pathological types, like adenocarcinoma and neuroendocrine carcinoma, may cause diagnostic difficulties

in clinical practice due to inexperience. Moreover, when it comes to cervical metastatic adenocarcinoma, diagnostic resection of salivary gland is not recommended even after thorough non-invasive investigations. Furthermore, salivary gland cancers show paucity of FDG avidity [32], which was proofed again in our study (patient 4 and 5). Some non-FDG radiopharmaceuticals, i.e., [^{18}F]Fluorothymidine ([^{18}F]FLT), [^{68}Ga]Ga-DOTA-Somatostatin Analogs ([^{68}Ga]Ga-DOTA-SSA), and [^{18}F]Fluoromisonidazole ([^{18}F]FMISO), are recommended to detect primary tumor of HNCUP [33]. However, these tracers are too specific to identify all types of head and neck cancers. Promisingly, recent studies have demonstrated [^{68}Ga]Ga-DOTA-FAPI-04 can evaluate a broad spectrum of malignancies, including adenocarcinoma, neuroendocrine carcinoma, and well-differentiated carcinoma and so on [23, 24]. In this study, [^{68}Ga]Ga-DOTA-FAPI-04 showed intensive uptake in submandibular gland (SUV_{max} = 16.50 and 15.80, respectively), providing sufficient information for following surgery. Notably, [^{68}Ga]Ga-DOTA-FAPI-04 had a higher detection rate in adenocarcinoma (2/2, 100%) than SCC (5/16, 31.25%) of HNCUP, which indicated [^{68}Ga]Ga-DOTA-FAPI-04 was more sensitive to adenocarcinoma. However, further research with larger sample size is needed to verify this result.

EBV and HPV infection strongly suggest the location (nasopharynx and oropharynx, respectively) of primary tumor of SCC HNCUP [34]. Gi Cheol Park et al [35] found that the sensitivity and accuracy of HPV were higher than those of [^{18}F]FDG PET/CT (71.4% vs. 49.2% and 85.2% vs. 68.5%, respectively). In the current cohort, primary tumors were detected in 3 of 6 HPV-positive patients, and 2 were palatine tonsil SCC and 1 was submandibular gland salivary ductal carcinoma. Thus, HPV may offer limited information when concerning various pathologic types rather than SCC. Furthermore, virus infection status can't provide direct anatomical information for further biopsy. With regard to the detection of regional and distant metastases, the performance of [^{68}Ga]Ga-DOTA-FAPI-04 PET/CT varies among different researches [24, 27]. In our study, [^{68}Ga]Ga-DOTA-FAPI-04 PET/CT showed similar performance ($p > 0.05$) with [^{18}F]FDG PET/CT in detecting both lymph node and bone metastases. Considering that radiation therapy is one of the most important modalities of treating HNCUP, the advantages of [^{68}Ga]Ga-DOTA-FAPI-04 PET/CT in both primary tumors and metastases may play a vital role in gross tumor volume delineation.

There are some limitations in this study. First, the main limitation is the relatively small number of patients, and the number of pathologic types is uneven. In the future, larger population cohort studies with more cancer types need to take into account. Second, not all the metastatic lymph nodes are confirmed by pathology. Nevertheless, imaging findings by both tracers and follow-up examinations can serve as a reference. Last, immunohistochemistry (IHC) for FAP expression of primary tumors and metastases is lacking. Hence, FAPI imaging and FAP expression control studies are also necessary in the future.

Conclusions

This study demonstrated that [^{68}Ga]Ga-DOTA-FAPI-04 PET/CT can improve the detection rate of primary tumor in HNCUP patients with negative FDG findings. Furthermore, with regard to the evaluation of metastatic lesions, [^{68}Ga]Ga-DOTA-FAPI-04 PET/CT showed similar performance with [^{18}F]FDG PET/CT. Since CUP (not limited to the head and neck) is in need of improved detection rate, future research containing more patients with CUP should be considered to evaluate the clinical value of [^{68}Ga]Ga-DOTA-FAPI-04 PET/CT in these patients.

Declarations

Funding information This work was funded by National Natural Science Foundation of China (Grant number 81771861, 81971648, and 81901778) and Shanghai Anticancer Association Program (Grant number HYXH2021004).

Authors' contributions All authors contributed to the study conception and design. Patients were enrolled by Xiaomin Ou, Zuguang Xia and Qing Guan. Material preparation, data collection and analysis were performed by Bingxin Gu, Xiaoping Xu, Ji Zhang and Silong Hu. The first draft of the manuscript was written by Bingxin Gu. The final manuscript was revised by Zhongyi Yang and Shaoli Song. All authors read and approved the final manuscript.

Compliance with ethical standards

Conflict of interest The authors declare that they have no conflict of interest.

Ethics approval All procedures involving human participants were carried out in accordance with the ethical standards of the institutional and/or national research committee and with the 1964 Helsinki Declaration and its later amendments or comparable ethical standards. This article does not contain any experiments with animals.

Consent to participate Informed consent was obtained from all individual participants included in the study.

Consent to publication Not applicable.

Availability of data and material Not applicable.

Code availability Not applicable.

References

1. Kennel T, Garrel R, Costes V, Boisselier P, Crampette L, Favier V. Head and neck carcinoma of unknown primary. Eur Ann Otorhinolaryngol Head Neck Dis. 2019;136(3):185-92. doi:10.1016/j.anorl.2019.04.002.
2. Network NCC. NCCN Guidelines for Treatment of Occult Primary (https://www.nccn.org/professionals/physician_gls/pdf/occult.pdf).
3. Maghami E, Ismaila N, Alvarez A, Chernock R, Duvvuri U, Geiger J et al. Diagnosis and Management of Squamous Cell Carcinoma of Unknown Primary in the Head and Neck: ASCO Guideline. J Clin Oncol. 2020;38(22):2570-96. doi:10.1200/jco.20.00275.
4. Galloway TJ, Ridge JA. Management of Squamous Cancer Metastatic to Cervical Nodes With an Unknown Primary Site. J Clin Oncol. 2015;33(29):3328-37. doi:10.1200/JCO.2015.61.0063.
5. Moy J, Li R. Approach to the Patient with Unknown Primary Squamous Cell Carcinoma of the Head and Neck. Curr Treat Options Oncol. 2020;21(12):93. doi:10.1007/s11864-020-00791-3.
6. Piazza C, Incandela F, Giannini L. Unknown primary of the head and neck: a new entry in the TNM staging system with old dilemmas for everyday practice. Curr Opin Otolaryngol Head Neck Surg. 2019;27(2):73-9. doi:10.1097/MOO.0000000000000528.
7. Keller LM, Galloway TJ, Holdbrook T, Ruth K, Yang D, Dubyk C et al. p16 status, pathologic and clinical characteristics, biomolecular signature, and long-term outcomes in head and neck squamous cell carcinomas of unknown primary. Head Neck. 2014;36(12):1677-84. doi:10.1002/hed.23514.

8. Junn JC, Soderlund KA, Glastonbury CM. Imaging of Head and Neck Cancer With CT, MRI, and US. Semin Nucl Med. 2021;51(1):3-12. doi:10.1053/j.semnuclmed.2020.07.005.
9. Regelink G, Brouwer J, de Bree R, Pruim J, van der Laan BF, Vaalburg W et al. Detection of unknown primary tumours and distant metastases in patients with cervical metastases: value of FDG-PET versus conventional modalities. Eur J Nucl Med Mol Imaging. 2002;29(8):1024-30. doi:10.1007/s00259-002-0819-0.
10. Freudenberg LS, Fischer M, Antoch G, Jentzen W, Gutzeit A, Rosenbaum SJ et al. Dual modality of 18F-fluorodeoxyglucose-positron emission tomography/computed tomography in patients with cervical carcinoma of unknown primary. Med Princ Pract. 2005;14(3):155-60. doi:10.1159/000084632.
11. Waltonen JD, Ozer E, Hall NC, Schuller DE, Agrawal A. Metastatic carcinoma of the neck of unknown primary origin: evolution and efficacy of the modern workup. Arch Otolaryngol Head Neck Surg. 2009;135(10):1024-9. doi:10.1001/archoto.2009.145.
12. Rusthoven KE, Koshy M, Paulino AC. The role of fluorodeoxyglucose positron emission tomography in cervical lymph node metastases from an unknown primary tumor. Cancer. 2004;101(11):2641-9. doi:10.1002/cncr.20687.
13. Zhu L, Wang N. 18F-fluorodeoxyglucose positron emission tomography-computed tomography as a diagnostic tool in patients with cervical nodal metastases of unknown primary site: a meta-analysis. Surg Oncol. 2013;22(3):190-4. doi:10.1016/j.suronc.2013.06.002.
14. Lee JR, Kim JS, Roh JL, Lee JH, Baek JH, Cho KJ et al. Detection of occult primary tumors in patients with cervical metastases of unknown primary tumors: comparison of (18)F FDG PET/CT with contrast-enhanced CT or CT/MR imaging-prospective study. Radiology. 2015;274(3):764-71. doi:10.1148/radiol.14141073.
15. Liu Y. FDG PET/CT for metastatic squamous cell carcinoma of unknown primary of the head and neck. Oral Oncol. 2019;92:46-51. doi:10.1016/j.oraloncology.2019.03.014.
16. Goel R, Moore W, Sumer B, Khan S, Sher D, Subramaniam RM. Clinical Practice in PET/CT for the Management of Head and Neck Squamous Cell Cancer. AJR Am J Roentgenol. 2017;209(2):289-303. doi:10.2214/ajr.17.18301.
17. Szyszko TA, Cook GJR. PET/CT and PET/MRI in head and neck malignancy. Clin Radiol. 2018;73(1):60-9. doi:10.1016/j.crad.2017.09.001.
18. Kuzet SE, Gaggioli C. Fibroblast activation in cancer: when seed fertilizes soil. Cell Tissue Res. 2016;365(3):607-19. doi:10.1007/s00441-016-2467-x.
19. Koczorowska MM, Tholen S, Bucher F, Lutz L, Kizhakkedathu JN, De Wever O et al. Fibroblast activation protein-alpha, a stromal cell surface protease, shapes key features of cancer associated fibroblasts through proteome and degradome alterations. Mol Oncol. 2016;10(1):40-58. doi:10.1016/j.molonc.2015.08.001.
20. Sanchez-Garrido MA, Habegger KM, Clemmensen C, Holleman C, Muller TD, Perez-Tilve D et al. Fibroblast activation protein (FAP) as a novel metabolic target. Mol Metab. 2016;5(10):1015-24. doi:10.1016/j.molmet.2016.07.003.
21. Rettig WJ, Garin-Chesa P, Beresford HR, Oettgen HF, Melamed MR, Old LJ. Cell-surface glycoproteins of human sarcomas: differential expression in normal and malignant tissues and cultured cells. Proc Natl Acad Sci U S A. 1988;85(9):3110-4. doi:10.1073/pnas.85.9.3110.
22. Scanlan MJ, Raj BK, Calvo B, Garin-Chesa P, Sanz-Moncasi MP, Healey JH et al. Molecular cloning of fibroblast activation protein alpha, a member of the serine protease family selectively expressed in stromal

fibroblasts of epithelial cancers. Proc Natl Acad Sci U S A. 1994;91(12):5657-61. doi:10.1073/pnas.91.12.5657.

23. Kratochwil C, Flechsig P, Lindner T, Abderrahim L, Altmann A, Mier W et al. (68)Ga-FAPI PET/CT: Tracer Uptake in 28 Different Kinds of Cancer. J Nucl Med. 2019;60(6):801-5. doi:10.2967/jnumed.119.227967.
24. Chen H, Pang Y, Wu J, Zhao L, Hao B, Wu J et al. Comparison of [(68)Ga]Ga-DOTA-FAPI-04 and [(18)F] FDG PET/CT for the diagnosis of primary and metastatic lesions in patients with various types of cancer. Eur J Nucl Med Mol Imaging. 2020;47(8):1820-32. doi:10.1007/s00259-020-04769-z.
25. Pang Y, Zhao L, Luo Z, Hao B, Wu H, Lin Q et al. Comparison of (68)Ga-FAPI and (18)F-FDG Uptake in Gastric, Duodenal, and Colorectal Cancers. Radiology. 2021;298(2):393-402. doi:10.1148/radiol.2020203275.
26. Syed M, Flechsig P, Liermann J, Windisch P, Staudinger F, Akbaba S et al. Fibroblast activation protein inhibitor (FAPI) PET for diagnostics and advanced targeted radiotherapy in head and neck cancers. Eur J Nucl Med Mol Imaging. 2020;47(12):2836-45. doi:10.1007/s00259-020-04859-y.
27. Serfling S, Zhi Y, Schirbel A, Lindner T, Meyer T, Gerhard-Hartmann E et al. Improved cancer detection in Waldeyer's tonsillar ring by (68)Ga-FAPI PET/CT imaging. Eur J Nucl Med Mol Imaging. 2021;48(4):1178-87. doi:10.1007/s00259-020-05055-8.
28. Lindner T, Loktev A, Altmann A, Giesel F, Kratochwil C, Debus J et al. Development of Quinoline-Based Theranostic Ligands for the Targeting of Fibroblast Activation Protein. J Nucl Med. 2018;59(9):1415-22. doi:10.2967/jnumed.118.210443.
29. Pencharz D, Dunn J, Connor S, Siddiqui A, Sriskandan N, Thavaraj S et al. Palatine tonsil SUVmax on FDG PET-CT as a discriminator between benign and malignant tonsils in patients with and without head and neck squamous cell carcinoma of unknown primary. Clin Radiol. 2019;74(2):165.e17-165.e23. doi:10.1016/j.crad.2018.10.007.
30. Redondo-Cerezo E, Martinez-Cara JG, Jimenez-Rosales R, Valverde-Lopez F, Caballero-Mateos A, Jervez-Puente P et al. Endoscopic ultrasound in gastric cancer staging before and after neoadjuvant chemotherapy. A comparison with PET-CT in a clinical series. United European Gastroenterol J. 2017;5(5):641-7. doi:10.1177/2050640616684697.
31. Spadafora M, Pace L, Evangelista L, Mansi L, Del Prete F, Saladini G et al. Risk-related (18)F-FDG PET/CT and new diagnostic strategies in patients with solitary pulmonary nodule: the ITALIAN multicenter trial. Eur J Nucl Med Mol Imaging. 2018;45(11):1908-14. doi:10.1007/s00259-018-4043-y.
32. Wong WL. PET-CT for Staging and Detection of Recurrence of Head and Neck Cancer. Semin Nucl Med. 2021;51(1):13-25. doi:10.1053/j.semnuclmed.2020.09.004.
33. Eisenmenger LB. Non-FDG Radiopharmaceuticals in Head and Neck PET Imaging: Current Techniques and Future Directions. Semin Ultrasound CT MR. 2019;40(5):424-33. doi:10.1053/j.sult.2019.07.006.
34. Civantos FJ, Vermorken JB, Shah JP, Rinaldo A, Suarez C, Kowalski LP et al. Metastatic Squamous Cell Carcinoma to the Cervical Lymph Nodes From an Unknown Primary Cancer: Management in the HPV Era. Front Oncol. 2020;10:593164. doi:10.3389/fonc.2020.593164.
35. Cheol Park G, Roh JL, Cho KJ, Seung Kim J, Hyeon Jin M, Choi SH et al. (18) F-FDG PET/CT vs. human papillomavirus, p16 and Epstein-Barr virus detection in cervical metastatic lymph nodes for identifying primary tumors. Int J Cancer. 2017;140(6):1405-12. doi:10.1002/ijc.30550.

Tables

Table 1. Patients' characteristics

Patient No.	Gender	Age (years)	EBV-DNA status	HPV status	p16 status	Pathologic type of cervical lymph node
1	M	52	P	U	U	SCC
2	M	63	N	P	P	SCC
3	M	58	N	P	P	SCC
4	M	50	N	U	U	AC
5	M	41	U	P	P	AC
6	M	55	N	U	U	SCC
7	M	54	N	N	N	SCC
8	M	72	N	U	U	SCC
9	M	61	N	P	N	SCC
10	M	47	N	N	P	SCC
11	M	62	N	N	N	SCC
12	F	55	P	N	N	SCC
13	M	63	N	U	U	SCC
14	F	67	N	U	U	SCC
15	M	40	N	P	P	SCC
16	M	24	N	N	N	SCC
17	M	55	N	U	U	SCC
18	M	51	U	P	P	SCC

M = male; F = female; P = positive; N = negative; U = unknown; SCC = squamous cell carcinoma; AC = adenocarcinoma

Table 2. Comparison of metastatic lesions on [^{18}F]FDG and [^{68}Ga]Ga-DOTA-FAPI-04 PET/CT in eighteen patients with HNCUP

Patient No.	Metastases		Range of metastases size (mm)	[^{18}F]FDG		[^{68}Ga]Ga-DOTA-FAPI-04		*p*-value	
	Location	No.		SUV_{max}	TBR	SUV_{max}	TBR	SUV_{max}	TBR
1	LN	3	7 - 8	5.27 ± 1.29	4.39 ± 1.07	2.27 ± 0.91	2.06 ± 0.82		
2	LN	2	7 - 20	6.55 ± 0.92	7.28 ± 1.02	7.10 ± 0.42	5.92 ± 0.35		
3	LN	2	10 - 16	8.10 ± 1.84	9.00 ± 2.04	14.40 ± 0.85	20.57 ± 1.21		
4	LN	16	7 - 22	10.78 ± 3.73	11.98 ± 3.48	13.69 ± 4.19	22.81 ± 6.98		
	Bone	1	N/A	8.00	8.89	18.20	30.33		
5	LN	8	4 - 8	2.70 ± 1.07	3.38 ± 1.33	9.41 ± 2.40	11.77 ± 3.00		
	Bone	1	N/A	8.60	10.75	20.20	25.25		
6	LN	2	17 - 22	5.60 ± 4.24	8.00 ± 6.01	5.35 ± 0.92	5.94 ± 1.02		
7	LN	1	17	7.60	8.44	12.80	14.22		
8	LN	1	38	25.60	36.57	15.20	19.00		
9	LN	4	7 - 17	15.78 ± 1.61	13.15 ± 1.34	3.83 ± 1.32	4.25 ± 1.47		
10	LN	1	27	7.30	9.13	3.1	2.58		
11	LN	2	13 - 20	15.35 ± 3.61	19.19 ± 4.51	5.60 ± 2.69	8.00 ± 3.84		
12	LN	3	13 - 21	10.80 ± 5.17	18.00 ± 8.62	5.63 ± 3.82	8.05 ± 5.46		
13	LN	1	10	6.20	8.86	8.60	9.56		
14	LN	8	5 - 11	6.81 ± 4.30	11.35 ± 7.17	7.60 ± 3.31	8.44 ± 3.68		
15	LN	1	5	2.10	2.63	2.90	3.63		
16	LN	3	12 - 26	12.63 ± 2.29	14.04 ± 2.55	11.87 ± 3.27	14.83 ± 4.08		

	Bone	15	N/A	8.08 ± 3.19	8.98 ± 3.55	5.33 ± 3.86	6.66 ± 4.83		
17	LN	3	10 - 19	8.80 ± 1.28	8.00 ± 1.16	7.60 ± 0.50	15.20 ± 1.00		
18	LN	4	4 - 18	11.08 ± 9.02	9.23 ± 7.52	7.58 ± 3.51	9.47 ± 4.39		
Sum	LN	65	4 - 26	9.05 ± 5.29	10.65 ± 6.59	9.08 ± 4.69	12.80 ± 8.11	0.975	0.100
	Bone	17	N/A	8.11 ± 3.00	9.08 ± 3.35	6.96 ± 5.87	9.14 ± 8.40	0.478	0.976

PET semiquantitative parameters were presented as means with standard deviation (SD); HNCUP = head and neck cancer of unknown primary; TBR = tumor-to-background ratio; LN = lymph node; N/A = not applicable

Table 3. Primary tumor characteristics and semiquantitative parameters of [^{68}Ga]Ga-DOTA-FAPI-04 PET/CT

Patient No.	TNM	Primary tumor location	Pathologic type	Tumor size (mm)	[^{68}Ga]Ga-DOTA-FAPI-04		
					SUV_{max}	TBR	SUV_{max} ratio
1	T1N1M0 Stage II	Nasopharynx top wall	NDSCC	6 ´ 5	2.60	2.36	2.17
2	T1N1M0 Stage I	Palatine tonsil right side	SCC	11 ´ 10	8.30	6.92	3.46
3	T1N1M0 Stage I	Palatine tonsil right side	SCC	13 ´ 10	11.50	16.43	8.21
4	T2N2M1 Stage IVC	Submandibular gland right side	SDC	23 ´ 20	16.50	27.50	4.58
5	T1N2M1 Stage IVC	Submandibular gland right side	SDC	17 ´ 13	15.80	19.75	6.87
6	T1N1M0 Stage III	Hypopharynx posterior wall	SCC	5 ´ 3	3.20	3.56	2.91
7	T1N1M0 Stage III	Sinus piriformis right side	SCC	6 ´ 5	3.60	4.00	3.27

TBR = tumor-to-background ratio; NDSCC = non-keratinizing differentiated squamous cell carcinomas; SCC = squamous cell carcinoma; SDC = salivary ductal carcinoma

Figures

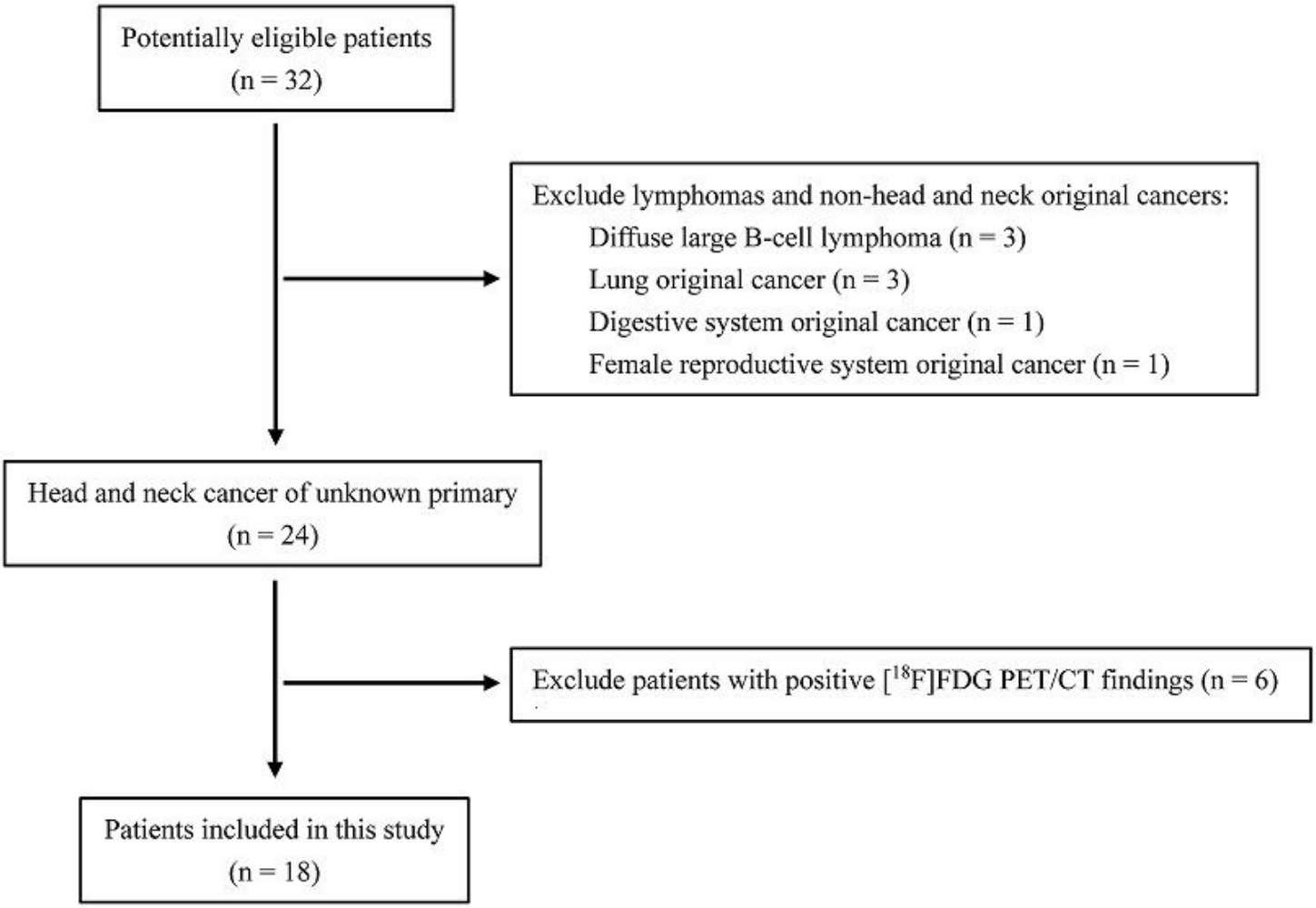

Figure 1

Flowchart of patient selection. * [68Ga]Ga-DOTA-FAPI-04 PET/CT could also identify the primary tumor in these patients.

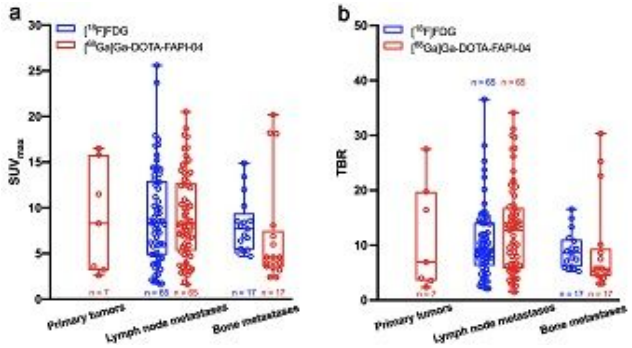

Figure 2

Boxplots of SUVmax (a) and TBR (b) on [18F]FDG versus [68Ga]Ga-DOTA-FAPI-04 PET/CT.

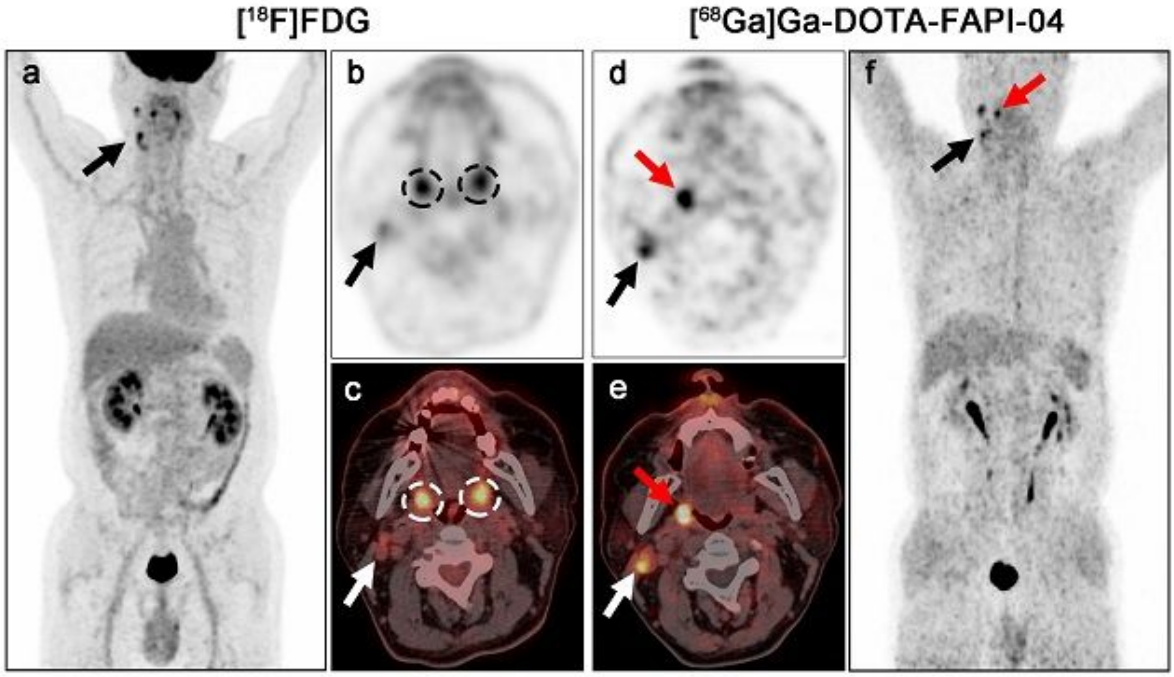

Figure 3

PET/CT scans with the [18F]FDG (a-c) and [68Ga]Ga-DOTA-FAPI-04 (d-f) in a 63-year-old male patient (patient 2) with metastatic squamous cell carcinoma (SCC) of the right neck. [18F]FDG PET/CT was negative for the detection of the primary. The increased uptake of FDG was detected in palatine tonsils of both right and left sides (b and c, black and white dashed circles; SUVmax = 6.40 and 6.00, respectively), resulting an SUVmax ratio of 1.07. On [68Ga]Ga-DOTA-FAPI-04 PET/CT, there was asymmetric fullness with intensive uptake in the right palatine tonsil (d-f, red arrow; SUVmax = 8.30), while low background uptake was seen in the left palatine tonsil (SUVmax ratio = 3.46). Subsequent tonsillectomy confirmed SCC. Black and white arrows indicate the metastatic lymph nodes.

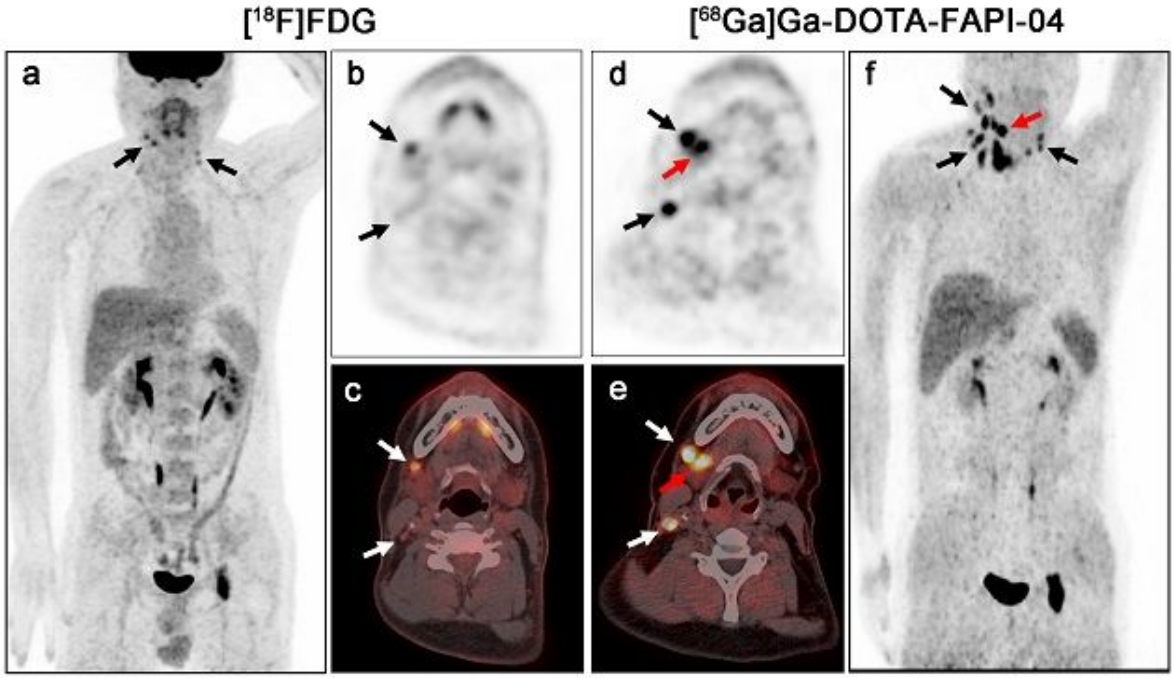

Figure 4

PET/CT scans with the [18F]FDG (a-c) and [68Ga]Ga-DOTA-FAPI-04 (d-f) in a 41-year-old male patient (patient 5) with metastatic adenocarcinoma of the right neck. [18F]FDG PET/CT was negative for the detection of the primary. On [68Ga]Ga-DOTA-FAPI-04 PET/CT, there was an intensive uptake in the right submandibular gland (d-f, red arrow; SUVmax = 15.80), while low background uptake was seen in the left submandibular gland (SUVmax ratio = 6.87). Subsequent surgery confirmed salivary ductal carcinoma. Black and white arrows indicate the metastatic lymph nodes.

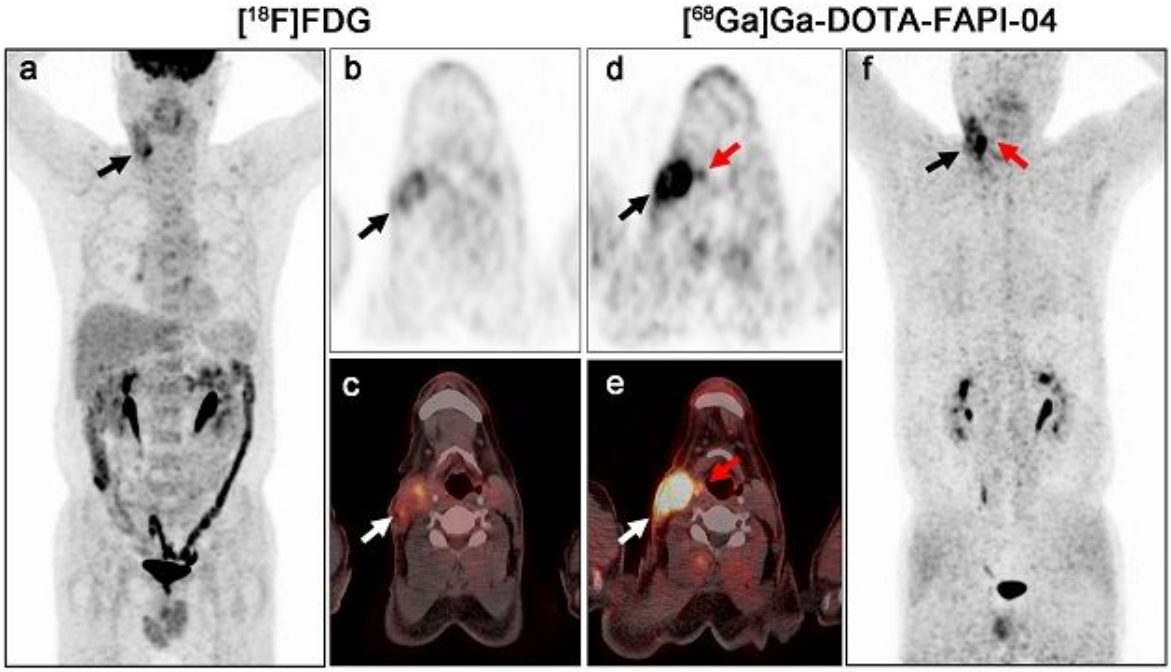

Figure 5

PET/CT scans with the [18F]FDG (a-c) and [68Ga]Ga-DOTA-FAPI-04 (d-f) in a 63-year-old male patient (patient 7) with metastatic squamous cell carcinoma (SCC) of the right neck. [18F]FDG PET/CT was negative for the detection of the primary. On [68Ga]Ga-DOTA-FAPI-04 PET/CT, there was a mild uptake in the right sinus piriformis (d-f, red arrow; SUVmax = 3.60), while low background uptake was seen in the left sinus piriformis (SUVmax ratio = 3.27). Subsequent biopsy confirmed SCC. Black and white arrows indicate the metastatic lymph node.